

## Studies of multibody charmless B decays at LHCb

---

**James MCCARTHY**<sup>\*†</sup>

*University of Birmingham*

*E-mail:* [jxm@hep.ph.bham.ac.uk](mailto:jxm@hep.ph.bham.ac.uk)

Recent results from studies of charmless  $B$  meson decays with the LHCb detector are presented.  $CP$  asymmetries in  $B^\pm \rightarrow K^\pm h^+ h^-$  decays have been measured and the first observation of  $CP$  asymmetry in inclusive three body charmless  $B$  meson decays is found in the  $B^\pm \rightarrow K^\pm K^+ K^-$  decays.  $CP$  asymmetries and dynamics in  $B^\pm \rightarrow p \bar{p} h^\pm$  decays have been measured, and we make the first observation of the  $B^+ \rightarrow \bar{\Lambda}(1520) p$  decay. Branching fractions of  $B_{(s)}^0 \rightarrow K_S^0 h^\pm h^\mp$  decays have been studied, including the first observation of the  $B_s^0 \rightarrow K_S^0 K^\pm \pi^\mp$  and  $B_s^0 \rightarrow K_S^0 \pi^+ \pi^-$  decays. No significant evidence for the  $B_s^0 \rightarrow K_S^0 K^+ K^-$  is observed and so a limit on this branching fraction is measured. Finally, the first preliminary results of the search for the  $\Lambda_b^0 \rightarrow \Lambda \eta'$  decay are presented. No significant signal is observed for this decay, and an upper limit is placed on the branching fraction.

*The European Physical Society Conference on High Energy Physics*

*18-24 July, 2013*

*Stockholm, Sweden*

---

<sup>\*</sup>Speaker.

<sup>†</sup>On behalf of the LHCb collaboration.

## 1. Introduction

Charmless  $B$  meson decays provide an interesting testing ground for the Standard Model, since they occur primarily through  $b \rightarrow s$  quark transitions, which are forbidden at tree level. Therefore, new physics contributions at loop level can affect the measured properties of such decays. This note presents the results of recent studies of multibody charmless  $B$  meson decays using data recorded by the LHCb detector [1] in 2011 and 2012.

## 2. $CP$ Violation in $B^\pm \rightarrow K^\pm h^+ h^-$ decays

This section summarises the recent analysis of the  $B^\pm \rightarrow K^\pm K^+ K^-$  and  $B^\pm \rightarrow K^\pm \pi^+ \pi^-$  decays using data recorded by the LHCb experiment, corresponding to an integrated luminosity of  $1.0 \text{ fb}^{-1}$  of  $pp$  collision data at a centre-of-mass energy of 7 TeV. Full details are described in Ref. [2]. This study is motivated largely by the  $CP$  violation observed in two body charmless  $B$  meson decays such as  $B^0 \rightarrow K^\pm \pi^\mp$  and  $B_s^0 \rightarrow K^\mp \pi^\pm$  decays [3]. The interference pattern exhibiting  $CP$  violating asymmetries involves a priori unknown strong phases. They are thought to be due to rescattering of hadrons in the final state (i.e.  $KK \rightarrow \pi\pi$ ), a process known as ‘‘compound  $CP$  violation’’ [4]. If this is the case, then the same effect should occur in  $B^\pm \rightarrow K^\pm K^+ K^-$  and  $B^\pm \rightarrow K^\pm \pi^+ \pi^-$  decays, and so these studies provide a good test of this hypothesis. We measure the  $CP$  asymmetries,

$$A_{CP}(B^\pm \rightarrow f^\pm) = \frac{\Gamma(B^- \rightarrow f^-) - \Gamma(B^+ \rightarrow f^+)}{\Gamma(B^- \rightarrow f^-) + \Gamma(B^+ \rightarrow f^+)}, \quad (2.1)$$

where  $\Gamma$  is the width of the decay, and  $f^\pm$  is the final state,  $K^\pm \pi^+ \pi^-$  or  $K^\pm K^+ K^-$ . By performing an unbinned maximum likelihood fit to the reconstructed  $B$  candidates, the raw asymmetry,  $A_{\text{raw}}$ , is extracted, where  $A_{\text{raw}} = A_{CP} + A_\Delta$ , and where  $A_\Delta = A_D(K^\pm) + A_P(B^\pm)$ , is the sum of the asymmetry in the detector efficiency of  $K^\pm$ ,  $A_D(K^\pm)$ , and the asymmetry in the production of  $B^\pm$ ,  $A_P(B^\pm)$ . For the  $B^\pm \rightarrow K^\pm \pi^+ \pi^-$  mode, the raw asymmetry is  $A_{\text{raw}}(K^\pm \pi^+ \pi^-) = 0.020 \pm 0.007$ , and for the  $B^\pm \rightarrow K^\pm K^+ K^-$  mode, the raw asymmetry is  $A_{\text{raw}}(K^\pm K^+ K^-) = -0.060 \pm 0.007$ . To extract  $A_{CP}$  from these values,  $A_\Delta$  is measured using a sample of  $B^\pm \rightarrow J/\psi(\mu^+ \mu^-)K^\pm$  decays, which has a similar topology to the signal decays, but has a negligible  $CP$  asymmetry which has been measured to be  $A_{CP}(J/\psi K) = (0.01 \pm 0.07)\%$  [5]. Using  $A_\Delta$  measured from this channel, the  $CP$  asymmetry is measured for each decay to be

$$\begin{aligned} A_{CP}(B^\pm \rightarrow K^\pm \pi^+ \pi^-) &= 0.032 \pm 0.008 \text{ (stat)} \pm 0.004 \text{ (syst)} \pm 0.007(A_{CP}(J/\psi K^\pm)), \\ A_{CP}(B^\pm \rightarrow K^\pm K^+ K^-) &= -0.043 \pm 0.009 \text{ (stat)} \pm 0.003 \text{ (syst)} \pm 0.007(A_{CP}(J/\psi K^\pm)). \end{aligned}$$

The significance of the asymmetry for the two decays modes is 2.8 standard deviations ( $\sigma$ ) and  $3.7\sigma$  respectively, and the latter is the first evidence of  $CP$  violation in inclusive three body charmless  $B$  meson decays.

In order to study the structure of the charge asymmetry in more detail, a Dalitz analysis is performed. Figure 1 shows the asymmetry of  $B^\pm$  events in two-dimensional bins of invariant mass, of  $m_{\pi\pi}^2$  vs  $m_{K^\pm \pi^\mp}^2$  for the  $B^\pm \rightarrow K^\pm \pi^+ \pi^-$  decay, and  $m_{K^+ K^- \text{ low}}^2$  against  $m_{K^+ K^- \text{ high}}^2$  for the  $B^\pm \rightarrow K^\pm K^+ K^-$  decay, where  $m_{K^+ K^- \text{ low}}^2 < m_{K^+ K^- \text{ high}}^2$ . In the  $B^\pm \rightarrow K^\pm \pi^+ \pi^-$  distribution, an

area of positive asymmetry is seen at low  $m_{\pi^+\pi^-}^2$ , around the  $\rho(770)$  resonance. The  $CP$  asymmetry is measured in the region  $0.08 < m_{\pi^+\pi^-}^2 < 0.66 \text{ GeV}^2/c^4$  and  $m_{K^\pm\pi^\mp}^2 < 15 \text{ GeV}^2/c^4$ , and is found to be  $A_{CP}^{\text{reg}}(B^\pm \rightarrow K^\pm\pi^+\pi^-) = 0.678 \pm 0.078 \text{ (stat)} \pm 0.032 \text{ (syst)} \pm 0.007(A_{CP}(J/\psi K^\pm))$ . In the  $B^\pm \rightarrow K^\pm K^+ K^-$  distribution, a localised region of negative asymmetry can be seen at low  $m_{K^+K^-}^2$  mass, not connected to any resonance. The  $CP$  asymmetry is measured in the region  $1.2 < m_{K^+K^-}^2 < 2.0 \text{ GeV}^2/c^4$  and  $m_{K^+K^-}^2 < 15 \text{ GeV}^2/c^4$ , and is  $A_{CP}^{\text{reg}}(B^\pm \rightarrow K^\pm K^+ K^-) = -0.226 \pm 0.020 \text{ (stat)} \pm 0.004 \text{ (syst)} \pm 0.007(A_{CP}(J/\psi K^\pm))$ .

### 3. $CP$ asymmetries and dynamics in $B^\pm \rightarrow p\bar{p}h^\pm$ decays

This section describes the study of the  $B^\pm \rightarrow p\bar{p}K^\pm$  and  $B^\pm \rightarrow p\bar{p}\pi^\pm$  decays [6], which are similar to the decays studied in the previous section. However, in this case, the rescattering of hadrons in the final state ( $hh \rightarrow p\bar{p}$ ) is not expected to play a large role, and hence gives complementary information to that obtained from  $B^\pm \rightarrow K^\pm K^+ K^-$  and  $B^\pm \rightarrow K^\pm\pi^+\pi^-$ . In addition to the  $CP$  asymmetry, the dynamics of each decay is investigated, by studying the differential production spectra as a function of three variables: the invariant mass of the  $p\bar{p}$  pair,  $m_{p\bar{p}}$ ; the invariant mass of the neutral combination of  $ph^-$  or  $\bar{p}h^+$ ,  $m_{(ph)^0}$ ; and the angle between this neutral combination in the  $p\bar{p}$  rest frame,  $\cos(\theta_p)$ . Figure 2 shows the differential production spectra for the two decays as a function of  $m_{p\bar{p}}$ . Each bin is corrected for the efficiency of that bin, and the charmonium resonances, corresponding to  $B^\pm \rightarrow J/\psi K^\pm$ ,  $B^\pm \rightarrow \eta_c K^\pm$ , and  $B^\pm \rightarrow \psi(2S)K^\pm$  for the  $B^\pm \rightarrow p\bar{p}K^\pm$  decay, and  $B^\pm \rightarrow J/\psi \pi^\pm$  for the  $B^\pm \rightarrow p\bar{p}\pi^\pm$  decay, are removed. The solid line shows the expected distribution assuming uniform phase space production, and an enhancement is observed at low  $m_{p\bar{p}}$ , corresponding to  $p\bar{p}$  scattering. Figure 3 shows the efficiency-corrected differential production yield as a function of  $m_{(pK)^0}$  for the  $B^\pm \rightarrow p\bar{p}K^\pm$  decay, showing only a small deviation from the phase space expectation in the range  $m_{(pK)^0} \in [4, 14] \text{ GeV}^2/c^4$ . No such deviation is seen in the  $B^\pm \rightarrow p\bar{p}\pi^\pm$  decay. Figure 4 shows the differential signal yield as a function of  $\cos(\theta_p)$ , and this is quantified by measuring the forward-backward asymmetry,  $A_{\text{FB}}$ , which describes the asymmetry between the number of events with a positive (negative) value of  $\cos(\theta_p)$ ,  $N_{\text{pos(neg)}}^{\text{RAW}}$

$$A_{\text{FB}} = \frac{N_{\text{pos}}^{\text{RAW}} - f \times N_{\text{neg}}^{\text{RAW}}}{N_{\text{pos}}^{\text{RAW}} + f \times N_{\text{neg}}^{\text{RAW}}}, \quad (3.1)$$

where  $f$  is the ratio of efficiencies for positive and negative  $\cos(\theta_p)$ ,  $f = \varepsilon_{\text{pos}}/\varepsilon_{\text{neg}}$ . The asymmetry is measured to be  $A_{\text{FB}}(p\bar{p}K^\pm) = 0.370 \pm 0.018 \text{ (stat)} \pm 0.016 \text{ (syst)}$  for the  $B^\pm \rightarrow p\bar{p}K^\pm$  decay and  $A_{\text{FB}}(p\bar{p}\pi^\pm) = -0.392 \pm 0.117 \text{ (stat)} \pm 0.015 \text{ (syst)}$  for the  $B^\pm \rightarrow \pi^\pm p\bar{p}$  decay. For the  $B^\pm \rightarrow p\bar{p}K^\pm$  decay, the  $CP$  asymmetry is studied using the same method described in Section 2, and is measured in different regions of  $p\bar{p}K$  invariant mass,  $m_{p\bar{p}K}$ . For the full  $m_{p\bar{p}}$  spectrum, the asymmetry is measured to be  $A_{CP}(p\bar{p}K^\pm) = -0.022 \pm 0.031 \text{ (stat)} \pm 0.007 \text{ (syst)}$ , while for low masses,  $m_{p\bar{p}K} < 2.85 \text{ GeV}/c^2$ ,  $A_{CP}(p\bar{p}K^\pm) = -0.047 \pm 0.036 \text{ (stat)} \pm 0.007 \text{ (syst)}$ . The asymmetry is also measured in two of the charmonium resonance regions, and no significant  $CP$  asymmetry is observed in any region, which is consistent with expectations, assuming the compound  $CP$  violation model.

Whilst studying the invariant mass spectra of this decay, a resonance is observed in the neutral  $Kp$  mass spectrum, which is found to correspond to the  $\Lambda(1520)$  baryon. This resonance is found to correspond to the  $B^+ \rightarrow \bar{\Lambda}(1520)p$  decay (plus the charge conjugated (cc) state), and Figure 5

shows the invariant mass of the  $Kp$  and the  $p\bar{p}K$  candidates. This is the first observation of this decay, with a significance of  $5.1\sigma$ . The branching fraction of this decay is measured relative to the  $B^+ \rightarrow J/\psi(p\bar{p})K^+$  normalisation channel, and is:

$$\mathcal{B}(B^+ \rightarrow \bar{\Lambda}(1520)p) = (3.9_{-0.9}^{+1.0}(\text{stat}) \pm 0.1(\text{syst}) \pm 0.3(\text{norm})) \times 10^{-7}. \quad (3.2)$$

#### 4. Branching fraction measurements of $B_{(s)}^0 \rightarrow K_S^0 h^\pm h^{\mp'}$ decays

This section describes updated measurements of the branching fraction of  $B^0 \rightarrow K_S^0 h^\pm h^{\mp'}$  decays, and the search for the  $B_s^0 \rightarrow K_S^0 h^\pm h^{\mp'}$  decays [7], where  $h=K, \pi$ . The analysis is performed using the 2011 dataset, and a boosted decision tree (BDT) is used to separate signal and background events. The candidates are categorised according to where in the LHCb detector the  $K_S^0$  meson decays. If the  $K_S^0$  meson decays before the silicon vertex detector, the event is categorised as a Long-Long (LL) event, and if the  $K_S^0$  meson decays downstream of the vertex detector, the event is categorised as a Down-Down (DD) event. Since the quality of the track information is different in each case, the selection must be optimised and applied separately to the two categories. As well as this, the BDT is optimised differently for the Cabibbo favoured modes and the Cabibbo suppressed modes. For the favoured modes, i.e. the  $B^0 \rightarrow K_S^0 K^+ K^-$ ,  $B_s^0 \rightarrow K_S^0 K^\pm \pi^\mp$  and  $B^0 \rightarrow K_S^0 \pi^+ \pi^-$  decays, a loose BDT selection is applied, and for the suppressed modes, i.e. the  $B_s^0 \rightarrow K_S^0 K^+ K^-$ ,  $B^0 \rightarrow K_S^0 K^\pm \pi^\mp$  and  $B_s^0 \rightarrow K_S^0 \pi^+ \pi^-$  decays, a tight BDT selection is applied. The invariant mass distribution for the final states with the loose BDT selection applied is shown in Figure 6. The middle plots show the unambiguous first observation of the  $B_s^0 \rightarrow K_S^0 K^\pm \pi^\mp$  decay. Figure 7 shows the results from the tight BDT selection. The left plots show no significant signal for the  $B_s^0 \rightarrow K_S^0 K^+ K^-$  decay. However, the right plots show the first observation of the  $B_s^0 \rightarrow K_S^0 \pi^+ \pi^-$  decay, and the significance of the signal from these categories combined is then  $5.9\sigma$ . The branching fraction of each decay is measured relative to the  $B^0 \rightarrow K_S^0 \pi^+ \pi^-$  decay. The Feldman-Cousins method [8] is used to place a limit on the branching fraction of the  $B_s^0 \rightarrow K_S^0 K^+ K^-$  decay, and the branching fractions have been measured to be

$$\begin{aligned} \mathcal{B}(B^0 \rightarrow K^0 K^\pm \pi^\mp) &= (6.4 \pm 0.9(\text{stat}) \pm 0.4(\text{syst}) \pm 0.3(\text{norm})) \times 10^{-6}, \\ \mathcal{B}(B^0 \rightarrow K^0 K^+ K^-) &= (19.1 \pm 1.5(\text{stat}) \pm 1.1(\text{syst}) \pm 0.8(\text{norm})) \times 10^{-6}, \\ \mathcal{B}(B_s^0 \rightarrow K^0 \pi^+ \pi^-) &= (14.3 \pm 2.8(\text{stat}) \pm 1.8(\text{syst}) \pm 0.6(\text{norm})) \times 10^{-6}, \\ \mathcal{B}(B_s^0 \rightarrow K^0 K^\pm \pi^\mp) &= (73.6 \pm 5.7(\text{stat}) \pm 6.9(\text{syst}) \pm 3.0(\text{norm})) \times 10^{-6}, \\ \mathcal{B}(B_s^0 \rightarrow K^0 K^+ K^-) &\in [0.2; 3.4] \times 10^{-6} \text{ at } 90\% \text{ CL}. \end{aligned}$$

#### 5. Search for the $\Lambda_b^0 \rightarrow \Lambda \eta'$ decay

This section describes the first preliminary results of the search for the  $\Lambda_b^0 \rightarrow \Lambda \eta'$  decay, using the 2012 data corresponding to an integrated luminosity of  $2.0 \text{ fb}^{-1}$  [9]. This decay has not been observed, but theoretical predictions are in the range  $\mathcal{B}(\Lambda_b^0 \rightarrow \Lambda \eta') \approx (1.8 - 19) \times 10^{-6}$  [10]. A BDT is used to select signal candidates, and Figure 8 shows the result of this selection for the LL and DD categories. No significant signal is obtained in either category, and so the Feldman-Cousins

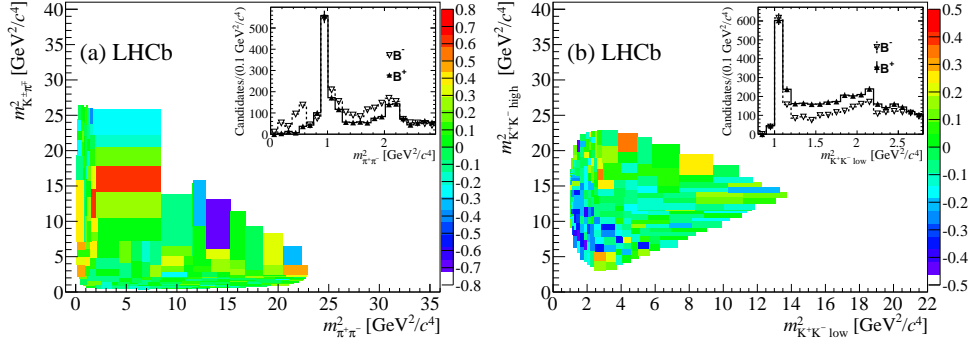


**Figure 1:**  $CP$  asymmetries in bins of the Dalitz plane for (a)  $B^\pm \rightarrow K^\pm \pi^+ \pi^-$  decays and (b)  $B^\pm \rightarrow K^\pm K^+ K^-$  decays. The inset figures show the projections of the number of background-subtracted events in bins of  $m_{\pi^+ \pi^-}^2$  for  $m_{K^\pm \pi^\mp}^2 < 15 \text{ GeV}^2/c^4$  and  $m_{K^+ K^- \text{ low}}^2$  for  $m_{K^+ K^- \text{ high}}^2 < 15 \text{ GeV}^2/c^4$

method is used to place an upper limit on the branching fraction relative to the  $B^0 \rightarrow K_S^0 \eta'$  decay. Using the known value of  $\mathcal{B}(B^0 \rightarrow K_S^0 \eta')$  the branching fraction is measured to be

$$\mathcal{B}(\Lambda_b^0 \rightarrow \Lambda \eta') < 6.2 \times 10^{-6} \text{ at } 90\% \text{ CL.} \quad (5.1)$$

## References

- [1] LHCb collaboration, A. A. Alves Jr. *et al.*, *The LHCb detector at the LHC*, *JINST* **3** (2008) S08005.
- [2] LHCb collaboration, R. Aaij *et al.*, *Measurement of  $CP$  violation in the phase space of  $B^\pm \rightarrow K^\pm \pi^+ \pi^-$  and  $B^\pm \rightarrow K^\pm K^+ K^-$* , *Phys. Rev. Lett.* **111** (2013) 101801, [arXiv:1306.1246](#).
- [3] LHCb collaboration, R. Aaij *et al.*, *First observation of  $CP$  violation in the decays of  $B_s^0$  mesons*, *Phys. Rev. Lett.* **110** (2013) 221601, [arXiv:1304.6173](#).
- [4] H.-Y. Cheng, C.-K. Chua, and A. Soni, *Final state interactions in hadronic  $B$  decays*, *Phys. Rev.* **D71** (2005) 014030, [arXiv:hep-ph/0409317](#).
- [5] Particle Data Group, J. Beringer *et al.*, *Review of particle physics*, *Phys. Rev.* **D86** (2012) 010001, and 2013 partial update for the 2014 edition.
- [6] LHCb collaboration, R. Aaij *et al.*, *Studies of the decays  $B^+ \rightarrow p \bar{p} h^+$  and observation of  $B^+ \rightarrow \bar{\Lambda}(1520) p$* , *Phys. Rev.* **D88** (2013) 052015, [arXiv:1307.6165](#).
- [7] LHCb collaboration, R. Aaij *et al.*, *Study of  $B_{(s)}^0 \rightarrow K_S^0 h^+ h^-$  decays with first observation of  $B_s^0 \rightarrow K_S^0 K^\pm \pi^\mp$  and  $B_s^0 \rightarrow K_S^0 \pi^+ \pi^-$* , [arXiv:1307.7648](#), to appear in JHEP.
- [8] G. J. Feldman and R. D. Cousins, *A Unified approach to the classical statistical analysis of small signals*, *Phys. Rev.* **D57** (1998) 3873, [arXiv:physics/9711021](#).
- [9] LHCb collaboration, *Search for the  $\Lambda_b^0 \rightarrow \Lambda \eta'$  decay at LHCb*, LHCb-CONF-2013-010.
- [10] M. Ahmady, C. Kim, S. Oh, and C. Yu, *Heavy baryonic decays of  $\Lambda_b^0 \rightarrow \Lambda \eta'$* , *Phys. Lett.* **B598** (2004) 203, [arXiv:hep-ph/0305031](#).

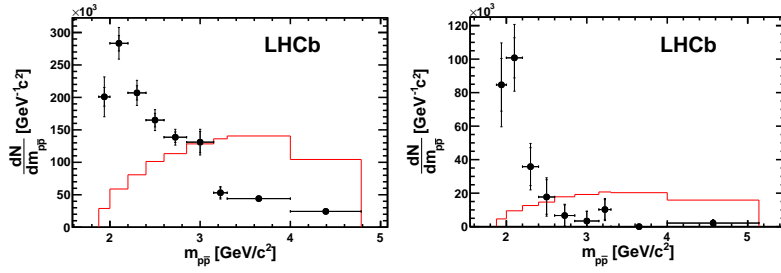


**Figure 2:** Differential production yields as a function of  $m_{p\bar{p}}$  for the  $B^{\pm} \rightarrow K^{\pm} p\bar{p}$  (left) and  $B^{\pm} \rightarrow \pi^{\pm} p\bar{p}$  (right) decays. For comparison, the expected distribution assuming uniform phase space production is shown as a solid line.

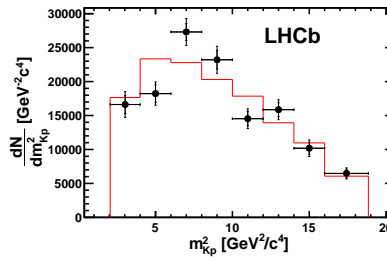


**Figure 3:** Differential production yields as a function of  $m_{(pK)^0}$  for the  $B^{\pm} \rightarrow K^{\pm} p\bar{p}$  decay. For comparison, the expected distribution assuming uniform phase space production is shown as a solid line.

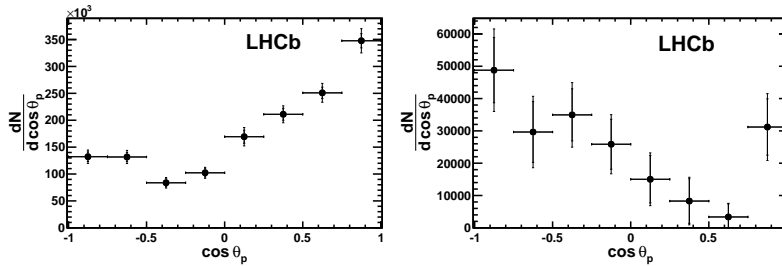


**Figure 4:** Differential production yields as a function of  $\cos(\theta_p)$  for the  $B^{\pm} \rightarrow K^{\pm} p\bar{p}$  (left) and  $B^{\pm} \rightarrow \pi^{\pm} p\bar{p}$  (right) decays.

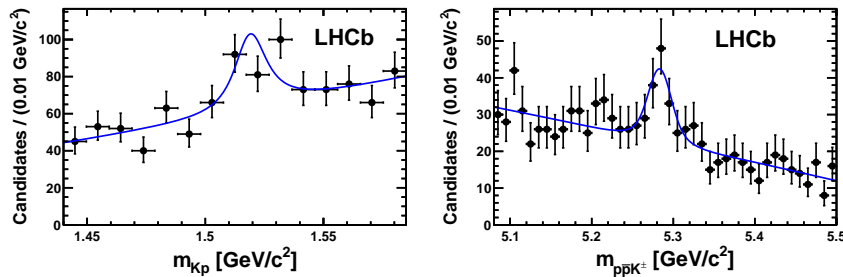


**Figure 5:** Invariant mass spectra of  $Kp$  candidates (left) and the  $p\bar{p}K$  candidates (right) for the  $B^+ \rightarrow \bar{\Lambda}(1520)p(+cc)$  decay.

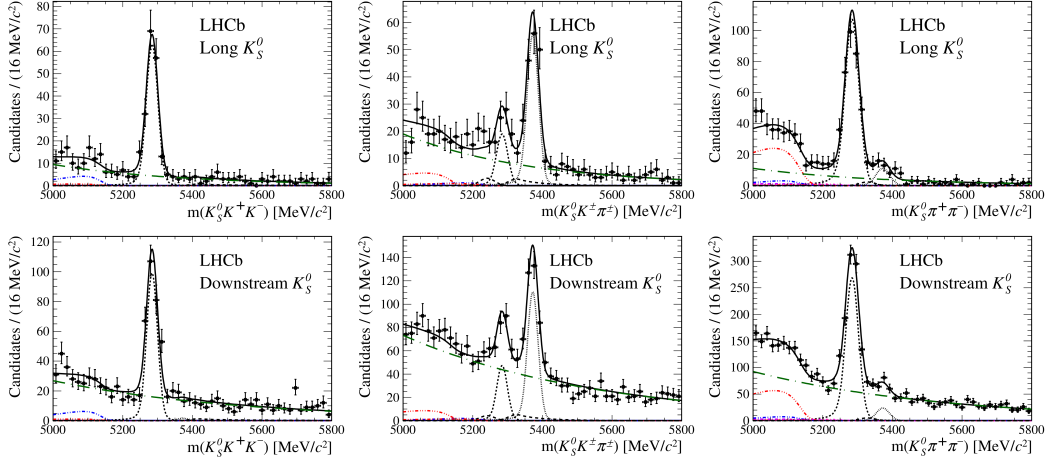


**Figure 6:** Invariant mass distribution of  $K_S^0 K^+ K^-$  (left),  $K_S^0 K^\pm \pi^\mp$  (middle) and  $K_S^0 \pi^+ \pi^-$  (right) obtained using the loose BDT selection for LL (top) and DD (bottom) category. The result of the fit is shown as the solid line overlaid.

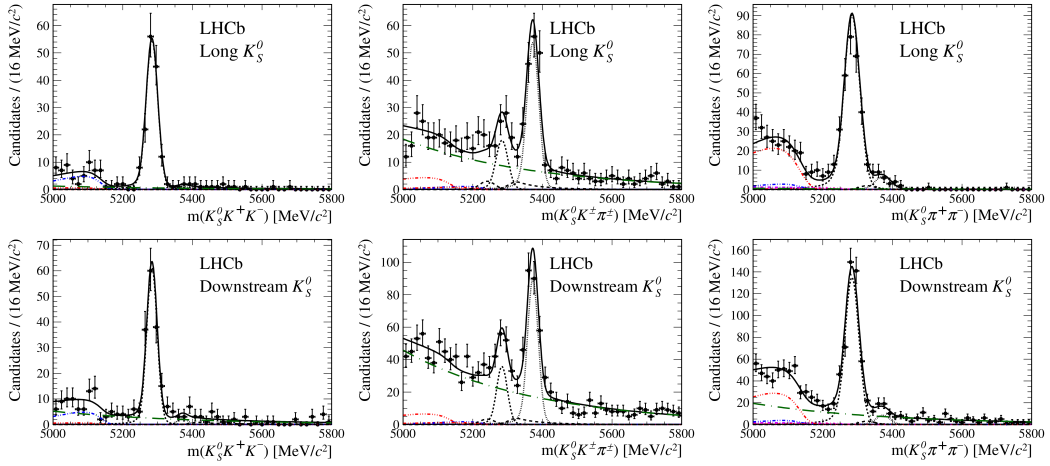


**Figure 7:** Invariant mass distribution of  $K_S^0 K^+ K^-$  (left),  $K_S^0 K^\pm \pi^\mp$  (middle) and  $K_S^0 \pi^+ \pi^-$  (right) obtained using the tight BDT selection for LL (top) and DD (bottom) category. The result of the fit is shown as the solid line overlaid.

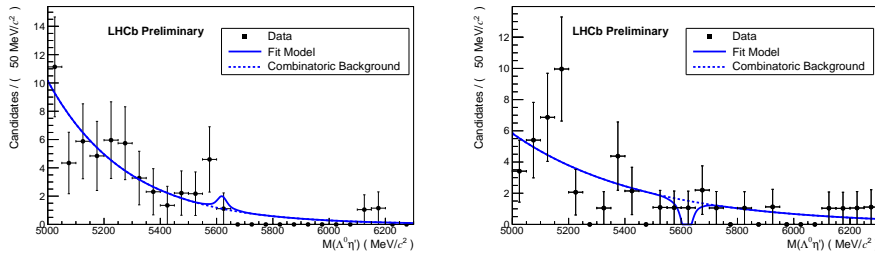


**Figure 8:** Invariant mass distribution of selected  $\Lambda_b^0$  candidates for the  $\Lambda_b^0 \rightarrow \Lambda \eta'$  decay, for the LL category (left) and the DD category (right).